Physica Scripta

PAPER

Enhancement of optoelectronic performance by plasmonic effect in TiO_2-rGO/Ag-TiO_2 based on UV detectors

RECEIVED
21 November 2024

REVISED
10 January 2025

ACCEPTED FOR PUBLICATION
16 January 2025

PUBLISHED
28 January 2025

Almar Zhumabekov, Talgat Dossanov, Assia Kassanova, Nurlybek Ispulov, Anargul Iskakova, Dilara Temirbayeva and Zhanat Daniyarova

Department of Physics, Mathematics, and Instrument Engineering, Toraighyrov University, Lomov Str., 64, Pavlodar, 140008, Kazakhstan

E-mail: almar89-89@mail.ru **and** dosts81@mail.ru

Keywords: reduced graphene oxide, titanium dioxide, nanocomposite material, UV photodetector, plasmon effect, NP Ag, "core-shell"

Abstract

This paper investigates the plasmonic effect in ultraviolet (UV) detectors based on titanium dioxide (TiO_2) and reduced graphene oxide (rGO). Studies have shown that a TiO_2-rGO nanocomposite material is obtained by hydrothermal synthesis. Adding silver nanoparticles (NPs) and Ag-TiO_2 'core-shell' nanostructures (NSs) leads to the plasmonic effect and an increase in the optoelectronic parameters. The TiO_2-rGO images were obtained with the help of SEM and Raman spectroscopy, and the ratio I_D/I_G was found. Hydrothermal synthesis results in a long-term reduction of rGO, i.e., the amount of oxygen-containing groups decreases. Raman spectroscopy shows the presence of peaks characteristic of the starting materials. The absorption properties when adding plasmonic nanoparticles to the films show changes in the absorption spectrum in the visible light region due to the transparency of rGO. The current-voltage characteristics show that the presence of plasmonic particles in the nanocomposite material leads to an increase in the photoinduced current of about 94 μA, which is almost 3.0 times greater. When irradiated, the multicomponent nanocomposite material with plasmonic nanoparticles responds to light three times faster than TiO_2- rGO. The results can be used to develop new light-sensitive devices for optoelectronic and photocatalytic applications.

1. Introduction

Recently, most electronic devices are directly or indirectly related to light interaction in various devices and applications. Photoreceiver or photodetectors that can effectively detect and measure incident light have attracted considerable attention. UV detectors are also used in such areas as fire radiation systems, military technologies, observations of space objects, and space communications, which require long-range data transmission and analysis of atmospheric pollution, water, soil, and pharmaceuticals [1–5]. Given this, UV detectors have become widespread due to their capabilities in various fields of application.

Ultraviolet radiation is used to analyze various substances since many molecules have characteristic absorption spectra in the ultraviolet range. This makes it possible to identify substances and investigate their composition and structures effectively identify substances and investigate their composition and structures.

Currently, significant research is focused on portable and highly sensitive UV detectors due to their rapid use in microelectronic devices.

Until now, many researchers have reported various photodetector mechanisms in the ultraviolet, visible, and IR regions. Thus, achieving excellent photoresponsibility and sensitive photodetector mechanism is primarily related to photoconductive, photoreflective, and photoelectric effects. As shown in [6], ultraviolet radiation is divided into four central spectral regions. It is known that UV light penetrates the Earth's atmosphere no more than 5%, and most of the UV radiation belongs to the UV–A category, i.e., from 400 to 320 nm.

Wide-bandgap semiconductor materials based on ZnO, SnO_2, Ga_2O_3, WO_3, and TiO_2 have proven UV-photoactive materials in optoelectronic devices [7–11]. TiO_2 is one of the most studied due to its potential.

Photocatalysis, solar cells, gas sensors, etc, are just a few applications. The absorption wavelength is in the range of 370–385 nm, and the bandgap width is in the region of 3.0–3.2 eV. TiO_2 is an excellent material for manufacturing a photodetector in the UV-A range. Thus, the properties of TiO_2 with excellent structural transformation and non-stoichiometric phase transitions ensure its importance in optoelectronic sensors and display systems [12, 13].

There are works in which the responsivity of the nanocomposite device was optimized with different nanostructures. Therefore, it makes sense to develop and study the combination and creation of a hybrid material to improve the properties of photodetectors [14, 15].

Graphene and its derivatives are already used in all areas of science, such as energy, photovoltaics, photoelectrochemical and photocatalytic generation of hydrogen and hydrocarbon fuels, and photodegradation of organic dyes [16–21].

The band gap can be controlled by manipulating the degree of oxidation of graphene oxide and changing the parameters of the sheets. The band gap of graphene oxide obtained in the work equals approximately ∼4.6 eV [22, 23]. Graphene oxide is often used in practice because it is more conveniently technologically obtained than graphene.

The study [24] considered nanocomposite materials synthesized by UV irradiation, hydrazine reduction, and hydrothermal methods. It was found that the nanocomposite material obtained by the hydrothermal method is highly effective as a photocatalyst for hydrogen extraction. Meanwhile, in [25], it was revealed that reduced graphene oxide has higher photocatalytic activity and electrical conductivity than graphene oxide. Hydrothermal synthesis is indeed an effective method for obtaining nanocomposite materials. This method allows you to control reaction conditions, such as temperature and pressure, which produce materials with specified properties. In synthesizing nanocomposites based on GO and TiO_2, the hydrothermal method can provide a more homogeneous distribution of components and improve the mechanical and electrical characteristics of the final product [26–29].

There are also well-known works on the interaction of graphene nanocomposites with plasmonic nanoparticles. For example, when interacting with Au and Ag nanoparticles, an increase in the luminescence of reduced graphene oxide is observed. It was suggested that plasmonic oscillations of Ag nanoparticles cause strong plasmon-exciton interaction and increase the radiative recombination of electron-hole pairs. It is shown that adding plasmonic nanoparticles improves the photocatalytic activity of the synthesized hybrid. Studies have shown that the photoluminescence and Raman scattering spectra on the surface of corrugated Ag films lead to an increase. It has been suggested that the amplification of optical signals occurs due to the scattering of surface plasmon-polariton modes on the metal film. Also, the plasmon effect can enhance the luminescence of graphene quantum dots. Studies of the influence of the plasmon effect are more widely used in the photocatalytic activity of semiconductors, photovoltaics, dye-sensitized solar cells, etc [30–37]. This effect can also be demonstrated and applied in the future in UV photodetectors. In this paper, we aim to investigate the optoelectronic characteristics of UV photodetectors by adding silver nanoparticles and observing the plasmon effect in nanocomposite materials.

2. Experiment

2.1. Materials

The following was used to prepare the multicomponent material: reduced graphene oxide (rGO, Cheaptubes) and TiO_2 (anatase, Sigma Aldrich), deionized water (purified by Drawel water purification system), ethanol (anhydrous, absolute), silver nitrate (Sigma Aldrich), titanium tetra isopropyl oxide (Sigma Aldrich), acetone (Sigma Aldrich), polyvinylpyrrolidone (AR grade), ethylene glycol, ethyl alcohol (reagent grade). The films were deposited into the surface of glass substrates coated with an FTO conductive layer (Fluorine-doped tin oxide coated glass slide, Sigma Aldrich). All reagents were analytically cleaned and used without additional cleaning.

2.2. Synthesis of nanocomposite materials TiO_2-rGO

Nanocomposite materials TiO_2-rGO were prepared with a concentration of carbonaceous material equal to 10 wt% titanium dioxide. The nanocomposite was prepared according to the method described in [38]. The mass ratio of rGO to TiO_2 was 10%. Previous works have shown that adding 10% rGO to TiO_2 is the optimal ratio.

The prepared paste is applied to the substrate's surface using the 'spin-coating' method. A rotation speed of 3000 rpm was selected to form thin films. After applying the paste, the film was annealed in an argon atmosphere for two hours at a temperature of 450 °C (Tmax).

2.3. Synthesis of nanocomposite materials TiO_2-rGO/Ag

0.5 g of polyvinylpyrrolidone was dissolved in 25 ml of ethylene glycol. The resulting mass was sonicated for 5 min and then vigorously stirred for 24 h. After the time had elapsed, 0.1 mmol (0.0169 g) of silver nitrate was added to the resulting solution and stirred until the salt was completely dissolved. The reaction flask was placed in a glycerol bath and vigorously stirred for 10 min at 40 °C, then 30 min at 120 °C. The result was a yellow-brown solution. The solution was divided evenly into 8 test tubes (test tube volume 15 ml); 10 ml of acetone was added to each test tube, shaken, and centrifuged for 40 min at 4000 rpm.

The acetone layer was drained, and the procedure was repeated. After draining the acetone layer, absolute ethyl alcohol was added at 3 ml and centrifuged for 20 min at 3600 rpm, and the alcohol layer was drained. The resulting silver nanoparticles were diluted with absolute ethyl alcohol to the desired concentration.

After the preparation of silver NPs, the 1 mg ml^{-1} solution was added to the powder of the nanocomposite material and left under stirring for 12 h. The concentration of Ag NPs in such pastes was equal to 10^{-13} mol L^{-1}. Studies [39] show that this concentration is the best for the enhanced plasmon effect, significantly improving the material's optical, catalytic, and detection properties.

2.4. Synthesis of nanocomposite materials TiO_2-rGO/Ag-TiO_2 NSs (core-shell)

To obtain silver nanoparticles (see 2.3), 2 ml of an ethanol solution of titanium triisopropyl oxide (7 μl in 1 ml) was added while cooling, stirred for 5 min, and then poured into 2 test tubes, placed in a rotator-shaker, and left for 24 h with constant shaking in a dark place.

After preparing nanocomposites with a plasmonic effect, a paste was prepared and applied to substrates, as shown in 2.2. The concentration of Ag NPs in such pastes was equal to 0.3% of the nanocomposite material. At this concentration, an enhanced plasmonic effect is also observed.

2.5. Characterization of samples

Images of the samples' surface morphology were obtained using the Mira 3MLU scanning electron microscope (Tescan). The Raman spectra were measured using a Confotec MR520 microscope (Sol Instruments) with a laser excitation wavelength of 532 nm. The films' absorption spectra were measured on quartz substrates using an ATP-2002 spectrophotometer (OptoSky). Suspensions of silver nanoparticles were measured on quartz cuvettes using a spectrofluorometer CM 2203 (Solar).

The samples' current-voltage characteristic (CVC) measurements were carried out using an impedance meter CS–350M (CorrTest). The samples were irradiated with a xenon lamp with a 35 mW cm^{-2} power. The substrate architecture was obtained using a 1610 RD150W (Bodor) laser machine.

2.6. The main characteristics

The key characteristics that ensure excellent performance of a photodetector are responsivity, detectivity, noise equivalent power, and external quantum efficiency. The importance of quality characteristics can be demonstrated independently of the film thickness, active area of the material, mechanism, architecture, and operating conditions. The key parameter for quantitative evaluation of the photocurrent generation per unit of illuminating radiation is the photodetector's responsivity. [6].

$$R = \frac{I_{light} - I_{dark}}{P} \tag{1}$$

Detectivity (D^*) is also an essential parameter for studying the effect of structure and material integration on the photodetector's performance. It is expected to improve the photodetector's overall performance. Detectivity can be estimated using the following expression.

$$D^* = \frac{R_\lambda \sqrt{A}}{\sqrt{(2eI_{dark})}} \tag{2}$$

Where—D^*, e, and I_{dark} are bandwidth, electronic charge, and dark current, respectively.

3. Results and discussion

Figures 1(a)–(c) shows SEM images of the nanocomposite material and the initial materials. Figure 1(c) shows that titanium dioxide nanoparticles are distributed uniformly on the surface of rGO sheets. Also, EDX analysis (figure 1(e)) confirms the presence of rGO in the nanocomposite material. SEM studies show the distribution of rGO throughout the volume of the synthesized nanocomposite materials. Such a distribution over the volume makes it possible to register photogenerated electrons. The architecture of the conductive substrate for applying

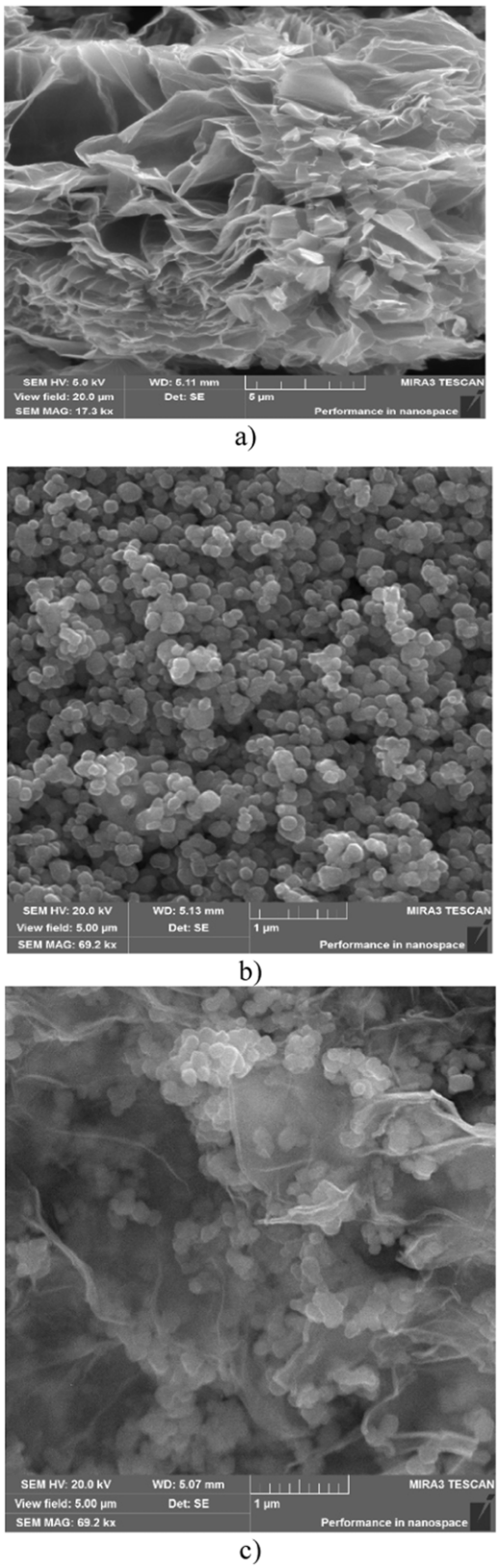

Figure 1. SEM images rGO, TiO_2, TiO_2-rGO (a)–(c), TEM image Ag-TiO_2 NSs (d) and EDX analysis nanocomposite material TiO_2-rGO (e).

the nanocomposite material is shown in figure 2. A line separating the surface of the layer into two poles was cut on the surface of the FTO glass using a laser scriber.

Research shows a photodetector's effectiveness depends on responsivity, detectivity, and quantum efficiency [6]. Despite this, the architecture of photodetectors can vary in shape and structure. However, the basis of all

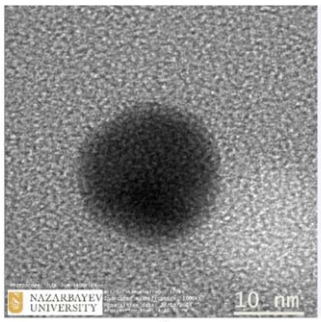

d)

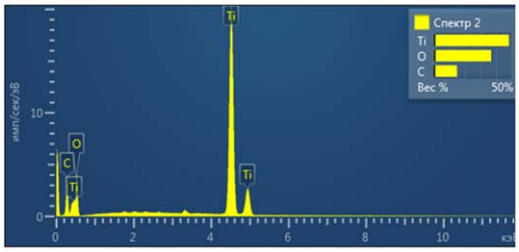

e)

Figure 1. (Continued.)

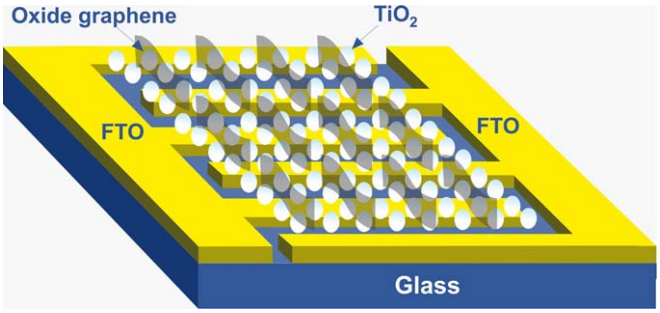

Figure 2. The scheme of the substrate photodetectors.

photodetectors is a substrate and a conductive layer that ensure their functionality. In this paper, the architecture looks like a substrate, a conductive layer, and a nanocomposite material applied to the surface, which makes it simpler and more technologically advanced.

Then, the TiO_2-rGO nanocomposite material and a paste with Ag NPs and Ag-TiO_2 NSs were applied to the FTO glass surface.

To confirm the reduction of graphene oxide during hydrothermal synthesis, Raman spectra of the synthesized samples were recorded (figure 3).

TiO_2 with the anatase structure has six combination-active peaks in the spectrum (figure 3). As shown in the figure, an intense and three medium bands are visible, corresponding to TiO_2. Eg(1) a peak of about 149 cm^{-1} is associated with Ti-O vibrations, Eg(2) about 183 cm^{-1} is associated with deformations and vibrations in the TiO_2 network, Eg(3) about 630 cm^{-1} may be related to more complex vibrations and combinations of vibrations in the structure. The two peaks, B1(1) 397 cm^{-1} and B1g(2) и 506 cm^{-1}—are responsible for Ti-O fluctuations and internal fluctuations in the structure, respectively. A1g is centered near 481 cm^{-1} and is associated with high-frequency oscillations [40].

Two bands, the D-band and the G-band, are observed in the Raman spectrum for rGO. These peaks are characteristic of graphene and its derivatives and are essential in analyzing structure and defects. The D-band is associated with defects in the rGO structure. The G-band is characteristic of all forms of graphene and an indicator of the quality and quantity of graphene layers [41].

In the spectrum of reduced graphene oxide, the D- and G-bands practically don't shift. This indicates a more significant number of defects in rGO that were formed due to the reduction of graphene oxide. The high ratio

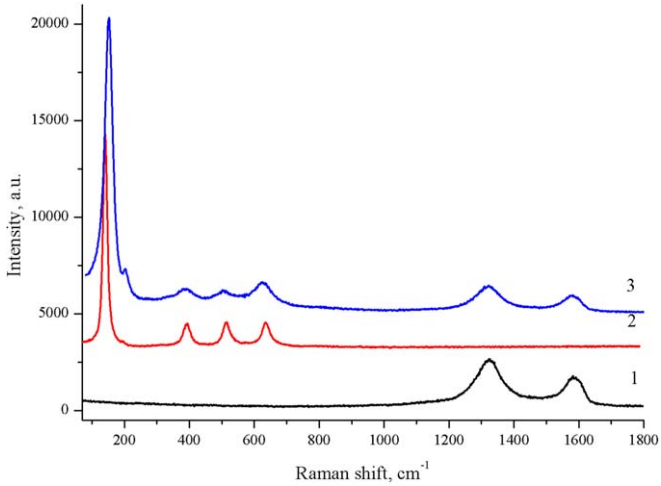

Figure 3. Raman shift rGO, TiO_2, TiO_2-rGO (1–3).

Table 1. Position and intensity of Raman bands.

Samples	D, cm^{-1}	I, a.u.	G, cm^{-1}	I, a.u.	I_D/I_G
rGO	1326.83	2708	1582.81	1789	1.51
TiO_2-rGO	1321.22	1584	1571.97	1079	1.47

between the heights of the D and G peaks is due to the high frequency of sp^2-domains in the carbon material. The position of the bands, the intensity, and the I_D/I_G ratio are shown in table 1.

The I_D/I_G ratio decrease also indicates a reduction in the functional groups in rGO. Thus, during the synthesis process, rGO continues to be further reduced by losing functional groups [28, 42, 43].

Within the study of the absorption spectrum of the nanocomposite, the data shown in figure 4 were obtained. The edge of the absorption band TiO_2 exhibits in the UV region of the spectrum of about 400 nm. The samples were applied to a thin layer of rGO to measure the absorption spectrum of rGO using an airbrush to a quartz substrate in a thin layer. The absorption spectrum of rGO has a maximum peak in the region of 230 nm and a weak peak at about 270 nm. RGO has a broad absorption band in the visible region of light. It also follows from figure 4 that TiO_2-rGO actively absorbs in the UV region, and it is also observed to be broadening into the visible region of light [25]. Thus, with the addition of rGO, it is possible to manufacture a nanocomposite material for absorption in the visible region. The addition of the Ag-TiO_2 NSs shows decreased absorption in the visible region. It is also noticeable that in the UV region, this nanocomposite has a shoulder in the region of 350 nm.

The long-wave shift of the TiO_2-rGO absorption band edge indicates a change in the band gap. This is because the addition of rGO can affect the electronic properties of TiO_2, which in turn leads to a change in its optical characteristics. Figure 4(b) shows the normalized absorption spectra of the synthesized Ag NPs and the Ag-TiO_2 NSs. The absorption spectrum of Ag NPs has a characteristic plasmon resonance band at 410 nm. When synthesizing Ag-TiO_2 NS of the core-shell composition, optical density increases due to the presence of TiO_2 NPs. According to the work, the core-shell dimensions correspond to 30–40 nm with this plasmon resonance [44, 45].

Further, the CVC photodetectors based on nanocomposite materials and TiO_2 were studied, which allowed us to estimate their optoelectronic characteristics.

The CVCs were measured from a positive voltage of +30 V to a negative value of −30 V. The I(U) dependence curves have a nonlinear shape. Moreover, high current values are recorded even without illumination of the samples (figure 5, a-c).

The CVC of the nanocomposite films shows that TiO_2-rGO, with the addition of Ag-TiO_2 NSs, has the highest generation of photoelectrons. The photoinduced current value for this nanocomposite is 93.586 μA. At the same time, the dark currents, which are 86.03 μA, also have high values. Next in decreasing photocurrent is TiO_2-rGO/Ag with the addition of Ag NPs with a concentration of 10^{-13} mol l^{-1}. As can be seen from table 1, the background current for all samples was calculated as the difference between the light and dark current. As can be seen from the figure, the sample with the addition of Ag-TiO_2 NSs has the highest value of the luminous

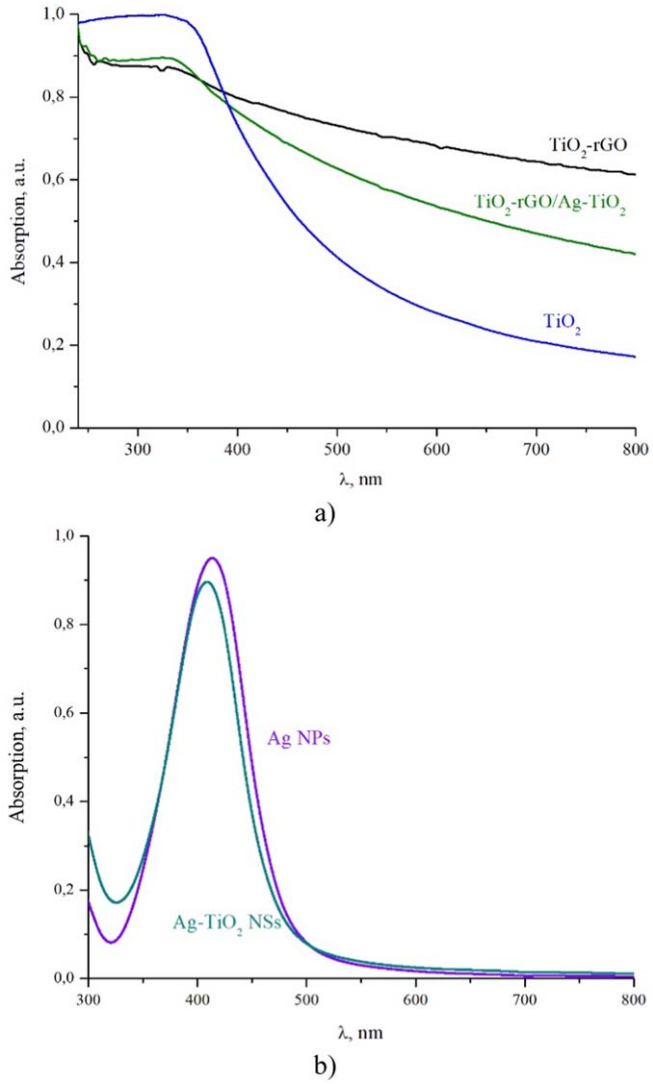

Figure 4. Absorption spectra samples.

current. Other samples almost do not differ and have a difference in light current of ~8 μA. This surge in current is most likely due to the Ag NPs, while dark currents also have high values. The Ag-TiO_2 NSs increase the light current by 2.8 and 3.0 times compared to other samples due to the plasmon effect. Due to the increase in the background current, R (equation (1)) has a high value and is almost 1.5 times greater. And D^* (equation (2)), in turn, is 1.3 times more than other samples. Table 2 shows in detail the optoelectronic parameters of these samples.

The latter parameters are key in photodetectors' general creation, assembly, and development. These indicators affect the high efficiency of the ultraviolet detector based on TiO_2 and rGO. Thus, the Ag-TiO_2 NSs show a better plasmonic effect than pure silver NPs. This is most likely due to the oxidation-reduction process of silver NPs. The shell in the structure 'protects,' and the oxidation-reduction process occurs slowly.

The negative voltage data show that the samples also show positive dynamics when irradiated with light. Negative photocurrent data correspond to the values obtained by applying positive voltage.

Introducing rGO into the TiO_2 matrix improves the photoelectric parameters of nanocomposites. This is explained by the fact that rGO has a high mobility of charge carriers, and electron transport occurs through effective paths. This contributes to an increase in the rate of charge separation. When adding plasmonic NPs to the nanocomposite, an improvement in conductivity is observed due to a decrease in resistance:

– rGO acts as a conductor that facilitates the movement of electrons;

– rGO creates a 'network' that improves the transfer of charge carriers to the pickup electrode;

– rGO promotes effective separation of electrons and holes, which reduces recombination.

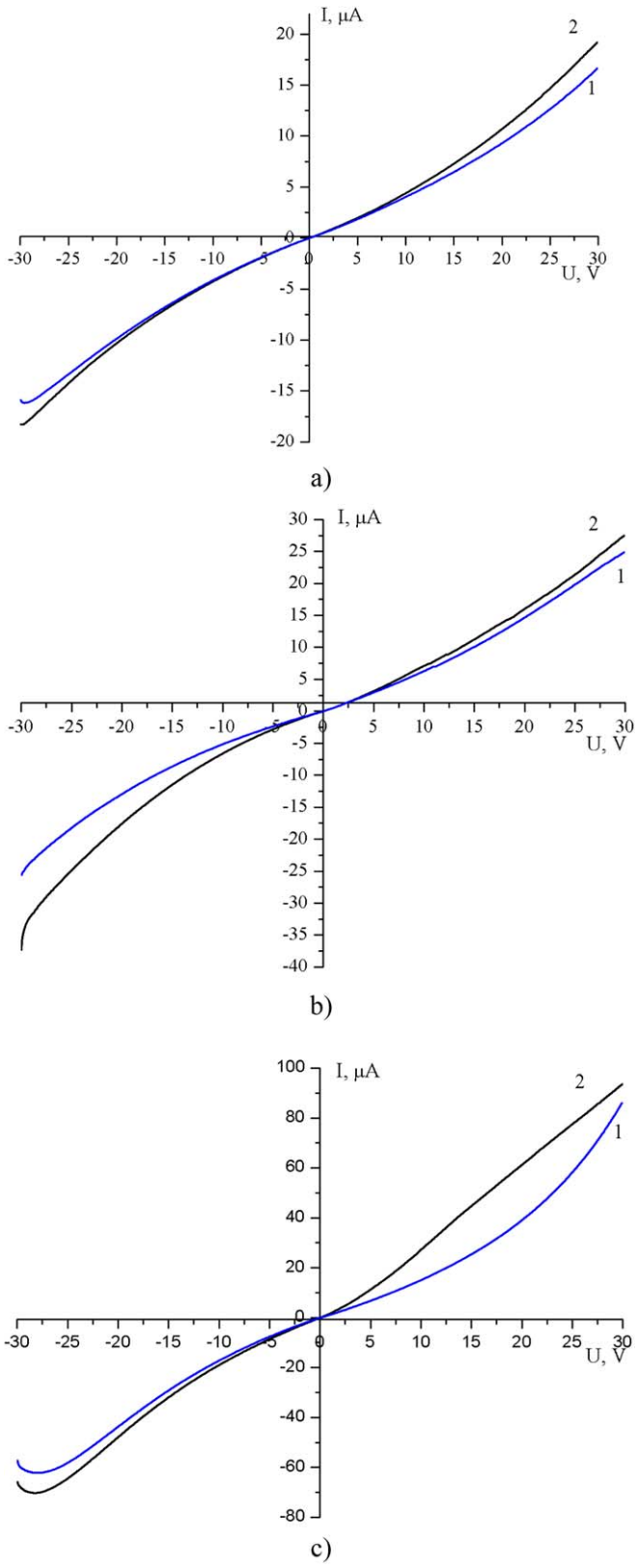

Figure 5. CVC photodetectors TiO_2-rGO (a), TiO_2-rGO/Ag (b) and TiO_2-rGO/Ag-TiO_2 (c): 1-dark, 2-light.

These data are consistent with the works [40, 45] and highlight the potential for using such nanocomposites in devices that require high conductivity and responsivity, such as photodetectors and solar cells.

Thus, it is clear that the addition of rGO to TiO_2 allows to reduce the resistance values of the semiconductor film by several times, which is consistent with the data of the authors of works [39, 46–48], where it was shown

Table 2. The photodetector characteristics.

Samples	I_L, μA	I_D, μA	I_{ph}, μA	R, μA/W	D*, Jones
TiO_2-rGO	19.19	16.658	2.532	72.3	$31.3^{*}10^{5}$
TiO_2-rGO/Ag	27.508	24.865	2.643	75.5	$26.76^{*}10^{5}$
TiO_2-rGO/Ag-TiO_2	93.586	86.03	7.556	215.9	$41.1^{*}10^{5}$

that this is achieved due to the movement of electrons through rGO sheets. In the presence of Ag NPs, an additional decrease in the resistance of the nanocomposite to electron transport is observed. The increase in the photoconductivity of titanium dioxide films in the presence of graphene oxide is also confirmed by the mobility of charge carriers in nanocomposites with and without Ag NPs.

4. Conclusion

Thus, a study was conducted on the influence of the plasmonic effect on the nanocomposite material to increase the efficiency of the UV detector. The plasmonic effect was expressed in two ways: in the form of silver NPs and Ag- TiO_2 NS of the 'core-shell' composition. The study of the morphology and structure showed that a nanocomposite material is formed during hydrothermal synthesis. TiO_2 NPs and a layered structure in the form of a 'ribbon' of rGO sheets are visible in SEM images. The EDX analysis shows the presence of chemical elements of the original materials in a percentage ratio. Also, rGO can be seen in the AFM image, which is visible as a 'ribbon.'

The addition of Ag NPs and Ag-TiO_2 NS of the 'core-shell' composition is confirmed by the absorption spectra and CVC of the samples. The absorption spectra show the production of Ag NPs and Ag- TiO_2 NSs. The CVC of the samples showed that the light photocurrents increase with the addition of the Ag-TiO_2 NSs by ~3.4 and ~4.9 times compared to TiO_2-rGO/Ag and TiO_2-rGO, respectively. The main optoelectronic parameters of the photodetector R and D* increase by ~2.8 and ~3.0 times and by 1.3 and 1.5 times, compared to TiO_2-rGO/Ag and TiO_2-rGO, respectively. Thus, a multicomponent nanocomposite material based on TiO_2 and rGO was synthesized and obtained in this work. The study's results showed high efficiency of the optoelectronic parameters of the UV detector with the addition of Ag-TiO_2 NSs. The plasmonic effect shows improved properties with a complex structure. At the same time, for Ag NPs, a 'protective' mechanism in the form of a shell is required for high efficiency.

Acknowledgments

This research is funded by the Science Committee of the Ministry of Science and Higher Education of the Republic of Kazakhstan (Grant No. AP19576361).

Data availability statement

All data that support the findings of this study are included within the article (and any supplementary files).

ORCID iDs

Almar Zhumabekov https://orcid.org/0000-0003-2360-3747
Nurlybek Ispulov https://orcid.org/0000-0003-4703-1413

References

[1] Wang Z L 2007 Novel nanostructures of ZnO for nanoscale photonics, optoelectronics, piezoelectricity, and sensing *Appl. Phys. Mater. Sci. Process* **88** 7–15
[2] Peng M *et al* 2016 Flexible self-powered GaN ultraviolet photoswitch with piezo-phototronic effect enhanced on/off ratio *ACS Nano* **10** 1572
[3] Yu X *et al* 2018 Narrow bandgap oxide nanoparticles coupled with graphene for high performance mid–infrared photodetection *Nat. Commun.* **9** 4299-1–4299-8
[4] Cheng R *et al* 2017 Ultrathin single-crystalline CdTe nanosheets realized via Van der Waals epitaxy *Adv. Mater.* **29** 1703122
[5] Yamada N, Kondo Y, Cao X and Nakano Y 2019 Visible-blind wide-dynamic-range fast-response self-powered ultraviolet photodetector based on CuI/In-Ga-Zn-O heterojunction *Appl. Mater. Today* **15** 153–62

[6] Omnes F, Monroy E, Munoz E and Reverchon J-L 2007 Wide bandgap UV photodetectors : A short review of devices and applications Gallium Nitride Materials and Devices II Vol. 6473 64730E-1-15 (https://doi.org/10.1117/12.705393)
[7] Rabani I *et al* 2021 Suppressed photocatalytic activity of ZnO based Core@Shell and RCore@Shell nanostructure incorporated in the cellulose nanofiber *Chemosphere* **269** 129311
[8] Chetri P and Dhar J C 2020 Improved photodetector performance of SnO_2 nanowire by optimized air annealing *Semicond. Sci. Technol.* **35** 045014
[9] Zhu W *et al* 2020 Influence of deposition temperature on amorphous Ga_2O_3 solar-blind ultraviolet photodetector *Semicond. Sci. Technol.* **35** 055037
[10] Liu J, Zhong M, Li J, Pan A and Zhu X 2015 Few-layer WO_3 nanosheets for high-performance UV-photodetectors *Mater. Lett.* **148** 184–7
[11] Cho H, Joo H, Kim H, Kim J E, Kang K S and Yoon J 2021 Improved photo-electrochemical properties of TiO_2 nanotubes doped with Er and effects on hydrogen production from water splitting *Chemosphere* **267** 129289
[12] Yan L, Yu J and Luo H 2017 Ultrafine TiO_2 nanoparticles on reduced graphene oxide as anode materials for lithium-ion batteries *Appl. Mater. Today* **8** 31–4
[13] Tang X S *et al* 2023 A self-powered ultraviolet photodetector based on TiO_2 nanoarrays and poly(3,4-ethylenedioxyselenophene) with the enhanced performance by pyro-phototronic effect *J. Alloys Compd.* **906** 170849
[14] Ahmad H *et al* 2018 Infrared photodetectors based on reduced graphene oxide nanoparticles and graphene oxide *Laser Phys.* **28** 066204-1–066204-8
[15] Kamat P V 2011 Graphene-based nanoassemblies for energy conversion *J. Phys. Chem. Lett.* **2** 242–51
[16] Wang D H, Choi D W, Li J, Yang Z G, Nie Z M and Kou R 2009 Self-assembled TiO_2-graphene hybrid nanostructures for enhanced Li-Ion insertion *ACS Nano* **3** 907–14
[17] Wang X, Zhi L and Muellen K 2008 Transparent, conductive graphene electrodes for dye-sensitized solar cells *Nano Lett.* **8** 323–7
[18] Zhumabekov A Z, Ibrayev N K, Seliverstova EV and Kamalova G B 2019 Preparation and study of electrophysical and optical properties of TiO_2-GO nanocomposite material *Bull. of the Univ. of Karag.-Phys.* **94** 54–60
[19] Ng Y H, Lightcap I V, Goodwin K, Matsumura M and Kamat P V 2010 To what extent do graphene scaffolds improve the photovoltaic and photocatalytic response of TiO_2 nanostructured films *J. Phys. Chem. Lett.* **15** 2222–7
[20] Ozer L Y, Garlisi C, Oladipo H, Pagliaro M, Sharief S A, Yusuf A, Almheiri S and Palmisano G 2007 Inorganic Semiconductors-Graphene Composites in Photo(electro)catalysis: synthetic strategies, interaction mechanisms and applications *J. Photochem. and Photobiol. C: Photochem. Rev.* **33** 132–64
[21] Phukan P and Sahu P P 2020 High performance UV photodetector based on metal-semiconductor-metal structure using TiO_2-rGO composite *Opt. Mater.* **109** 110330–9
[22] Zhu S, Song Y, Zhao X, Shao J, Zhang J and Yang B 2015 The photoluminescence mechanism in carbon dots (graphene quantum dots, carbon nanodots, and polymer dots): current state and future perspective *Nano Res.* **8** 355–81
[23] Tian P, Tang L, Teng K S and Lau S P 2018 Graphene quantum dots from chemistry to applications *Materials Today Chemistry* **10** 221–58
[24] Fan W, Lai Q, Zhang Q and Wang Y 2011 Nanocomposites of TiO_2 and reduced graphene oxide as efficient photocatalysts for hydrogen evolution *J. Phys. Chem.* C **115** 10694–701
[25] Ibrayev N, Zhumabekov A, Ghyngazov S and Lysenko E 2019 Synthesis and study of the properties of nanocomposite materials TiO_2-GO and TiO_2-rGO *Material Research Express* **6** 1–11
[26] Zhang Y, Tang Z-R, Fu X and Xu Y 2010 TiO_2-graphene nanocomposites for gas-phase photocatalytic degradation of volatile aromatic pollutant: is TiO_2-graphene truly different from other TiO_2-carbon composite materials? *ACS Nano* **4** 7303–14
[27] Seliverstova E, Serikov T, Ibrayev N and Sadykova A 2021 Synthesis, structure, and physical properties of a nanocomposite based on graphene oxide and TiO_2 *Russ. J. Phys. Chem.* A **95** 747–53
[28] Zhang D *et al* 2015 Enhanced performance of a TiO_2 ultraviolet detector modified with graphene oxide *RSC Adv.* **102** 83795–800
[29] Serikov T M, Ibrayev N K, Ivanova T M and Savilov S V 2021 Influence of the hydrothermal synthesis conditions on the photocatalytic activity of titanium dioxide nanorod *Inorganic Synthesis and Industrial Inorganic Chemistry* **94** 442–9
[30] Wang T, Tang T, Gao Y, Chen Q, Zhang Z and Bian H 2019 Hydrothermal preparation of Ag-TiO_2-reduced graphene oxide ternary microspheres structure composite for enhancing photocatalytic activity *Physica E* **112** 128–36
[31] Serikov T M, Zhanbirbayeva P A, Baltabekov A S and Kuanyshbekova A B 2022 Photocatalytic activity of the TiO_2/Ag/rGO nanocomposite *Bulletin of the University of Karaganda-Physics* **108** 14–21
[32] Seliverstova E, Serikov T, Nuraje N, Ibrayev N, Sadykova A and Amze M 2024 Plasmonic effect of metal nanoparticles on the photocatalytic properties of TiO_2/rGO composite *Nanotechnology* **35** 325401
[33] Lee J-H *et al* 2015 Photocatalytic Performance of Graphene/Ag/TiO2 Hybrid Nanocomposites *Carbon letters* **16** 247–54
[34] Tian H, Wan C, Xue X, Hu X and Wang X 2017 Effective electron transfer pathway of the ternary TiO_2/RGO/Ag nanocomposite with enhanced photocatalytic activity under visible light *Catalysts* **7** 1–15
[35] Gao W, Wang M, Ran C, Yao X, Yang H, Liu J, He D and Bai J 2014 One-pot synthesis of Ag/r-GO/TiO_2 nanocomposites with high solar absorption and enhanced anti-recombination in photocatalytic applications *Nanoscale* **6** 5498
[36] Afanasyev D A, Ibrayev N K, Serikov T M and Zeinidenov A K 2016 Effect of the titanium dioxide shell on the plasmon properties of silver nanoparticles *Russ. Jour. of Phys. Chem.* A **90** 833–7
[37] Sahu S K, Reddy S K, Singh M and Avrutin E 2022 Hybrid plasmonic waveguide based platform for refractive index and temperature sensing *IEEE Photonics Technol. Lett.* **34** 953–6
[38] Zhumabekov A Z, Ibrayev N K and Seliverstova E V 2020 Photoelectric properties of a nanocomposite derived from reduced graphene oxide and TiO_2 *Theor. Exp. Chem.* **55** 398–406
[39] Seliverstova E, Zhumabekov A and Ibrayev N 2020 The effect of silver nanoparticles on the photodetecting properties of the TiO_2/graphene oxide nanocomposite *Opt. Spectrosc.* **128** 1337–45
[40] Swamy V, Kuznetsov A, Dubrovinsky L S, Caruso R A, Shchukin D G and Muddle B C 2005 Finite-size and pressure effects on the Raman spectrum of nanocrystalline anatase TiO_2 *Phys. Rev.* B **71** 184302–12
[41] Ferrari A C *et al* 2006 Raman spectrum of graphene and graphene layers *Phys. Rev. Lett.* **97** 187401–4
[42] Laurenti M, Lamberti A, Genchi G G, Roppolo I, Canavese G, Vitale-Brovarone C, Ciofani G and Cauda V 2018 Graphene oxide finely tunes the bioactivity and drug delivery of mesoporous ZnO scaffolds *ACS Appl. Mater. Interfaces* **11** 449–56
[43] Dzhanabekova R K, Seliverstova E V, Zhumabekov A Z and Ibrayev N K 2019 Fabricating and examining of langmuir films of reduced graphene oxide *Rus. Jour. of Phys. Chem.* A **93** 338–42

[44] Alikhaidarova E, Afanasyev D and Ibrayev N 2020 Electrical properties of nanocomposite materials based on PEDOT:PSS polymer mixture doped with Ag, Ag-TiO_2 and Ag-SiO_2 nanoparticles *Mater. Today Proc.* **25** 28–32
[45] Angkaew S and Limsuwana P 2012 Preparation of silver-titanium dioxide core-shell (Ag@TiO_2) nanoparticles: effect of Ti-Ag mole ratio *Procedia Engineering* **32** 649–55
[46] Patil V, Capone A, Strauf S and Yang E H 2013 Improved photoresponse with enhanced photoelectric contribution in fully suspended graphene photodetectors *Sci. Rep.* **3** 2791
[47] He T *et al* Solar–blind ultraviolet detection based on TiO_2 nanoparticles decorated graphene field–effect transistors *Nanophotonics* **8** 899–908
[48] Kim S H *et al* 2018 Fabrication and optimization of the thermally treated titanium dioxide thin film-based ultraviolet photodetectors *Semicond. Sci. Technol.* **33** 015020